Ab initio electronic-structure calculations on the Au/Ag multilayer system and Au epitaxy on the Ag(110) surface

H. van Leuken and A. Lodder
Faculteit Natuurkunde en Sterrenkunde, Vrije Universiteit, De Boelelaan 1081, 1081 HV Amsterdam, The Netherlands

R. A. de Groot
Research Institute of Materials, Katholieke Universiteit Nijmegen, Toernooiveld 1, 6525 ED Nijmegen, The Netherlands
(Received 3 May 1991)

Ab initio electronic-structure calculations are performed for Au/Ag multilayers with small modulation wavelengths in the [100], [110], and [111] fcc modulation directions and for Ag [110] slabs covered with none, one, two, or three Au(110) layers. The total energies of the multilayers can be ordered according to the number of Au-Ag nearest-neighbor pairs in these systems, from which the bonding at the interface can be estimated. The multilayer and slab results taken together allow for a decomposition of the energetics of Au adlayer behavior on the Ag(110) surface. It is found that a bare Ag(110) surface is energetically more favorable than an Ag(110) surface covered by Au monolayers. This is in agreement with the difference in surface energy of Au and Ag surfaces, and it implies that the bonding energy gained at the Au-Ag interface is insufficient to overcome this difference. Therefore Au will tend to grow in islands on an Ag(110) surface rather than wetting it. Our results, based on Au-Ag bonding and the open geometry of the Ag(110) surface, support the bilayer-growth model that has recently been reported in the literature, but this support is only for the first two layers in the islands. Whereas the density-of-states (DOS) curves of the multilayers show hardly any variation for the different systems, the layer-resolved densities of states for the slabs show pronounced changes on going from the surface layers inward. For all slabs, with or without Au atop, an interface state can be observed, localized between the first and second surface layer. Furthermore, a shift in the *d*-state density to higher energies at the interface and to lower energies for the layer below the interface occurs as compared with the elemental DOS curves.

I. INTRODUCTION

Because of the structural and electronic similarity of the metals Au and Ag, it is expected that they can be combined easily by sputtering and evaporation techniques, thus forming an ideal model system for studies in the field of thin films and metallic superlattices. Therefore, the epitaxy of Au on Ag and vice versa has been studied extensively over the past years[1–3] and remains of interest. As for the epitaxy of Au on different Ag surfaces, different growth modes have been reported. For instance, the growth of Au on Ag(111) was found to follow the Frank–van der Merwe mode, characterized by an ideal layer-by-layer growth.[3] Recently another mode was reported by Fenter and Gustafsson[4,5] concerning the growth of Au on Ag(110). It was demonstrated that Au prefers to grow in a bilayer Volmer-Weber mode, which is characterized by two-dimensional islanding.

The very small lattice-parameter mismatch between Au and Ag, being less than 0.2%, and the fact that diffusion of Au into the Ag substrate is negligible at or below room temperature,[3] allow for a very simple, strainless, Au-Ag interface. Therefore, the assumption of ideal interfaces, as often used in band-structure calculations, is perfectly realized for this system. This makes this system also attractive for electronic-structure calculations, which are the subject of this paper. The localized-spherical-wave (LSW) method[6] was used, an all-electron self-consistent-field method where the same approximations are employed as in the more familiar augmented-spherical-wave (ASW) method of Williams, Kübler, and Gelatt[7] but which is devised to handle systems with a large number of atoms per unit cell.

We first consider calculations for coherent (lattice matched) Au/Ag multilayers in the [100], [110], and [111] modulation directions. We restrict ourselves to modulations with equal numbers of Au and Ag layers. The number of layers of each metal is at most three. Density-of-states curves and total-energy results for these systems will be presented and discussed in Secs. IV A and IV B, respectively.

The second part of this work is concerned with the growth mode reported by Fenter and Gustafsson. For this purpose calculations on [110] slabs, modeled by metal-vacuum multilayers, are performed for Ag slabs covered by three or less Au layers, including the uncovered Ag surface. The density-of-states curves for these systems will be presented and discussed in Sec. V. The energetics form the subject of Sec. VI.

Section II describes the unit cells and Sec. III gives the computational details. Concluding remarks are made in Sec. VII.

II. UNIT CELLS

The underlying structure used for all calculations, both on multilayers and slabs, is the fcc structure with a lattice

parameter of 4.085 Å. This value differs only 0.12% from the values of the bulk metals which are 4.09 Å for Ag and 4.08 Å for Au. The unit cells of the Au/Ag multilayers are constructed straightforwardly by stacking (100), (110), or (111) fcc planes. We have only considered multilayers with equal numbers n of planes for both metals only, with a maximum of $n=3$, and denote them as n:n. Neglecting interdiffusion, the cells can be chosen to contain only one atom per layer. Unit cells for the different modulation directions are depicted in Fig. 1. The [100] multilayers with larger modulation wavelengths are constructed by simply adding the units of Fig. 1(a) and scaling of the c axes by n. This approach cannot be followed for the [110] direction, where the larger cells are taken as orthorhombic with dimensions $(\frac{1}{2}a\sqrt{2}, a, n\times\frac{1}{2}a\sqrt{2})$. All [111] cells are trigonal, but the larger-modulation-wavelength cells have hexagonal axes instead of the rhombohedral axes for the 1:1 cell. For the determination of the length of the unit-cell c axis, the commensuration of the stacking with the concentration profile has to be taken into account. The fcc [111] stacking ABC is only commensurate with the 2:2 multilayers when four cubes are used, by which the c-axis length becomes $4a\sqrt{3}$ in the 2:2 [111] system. For this cell the first layer has $z=\frac{1}{24}$ and the inversion center occupies the Wyckoff 1b position. The c-axis unit-cell length of the 3:3 [111] multilayer in Fig. 1(c) is only half of the c-axis length of the 2:2 [111] system because now there is already commensuration when two cubes are used.

The semi-infinite solid is frequently modeled by a slab, a system that also has translational symmetry in two dimensions, now with two metal-vacuum interfaces. The calculational method we are using requires translational symmetry in three dimensions. This condition was fulfilled by simulating a slab by a metal-vacuum multilayer configuration. The slabs are constructed by stacking fcc (110) layers which results in a cell with the same symmetry (orthorhombic) as the one for the [110] 3:3 multilayer. The structures thus found will, for the sake of briefness, be referred to as slabs also. For the pure Ag slab we used a cell containing 14 layers—9 metal and 5 vacuum layers—with 8 classes. For the Au-covered slabs a total number of 20 layers was used, described by 11 classes. The number of vacuum layers was kept constant and equal to five. In increasing the number of Au layers the number of Ag layers was decreased. As an example, the unit cell of the Ag slab covered with 3 Au layers on either side is given in Fig. 2.

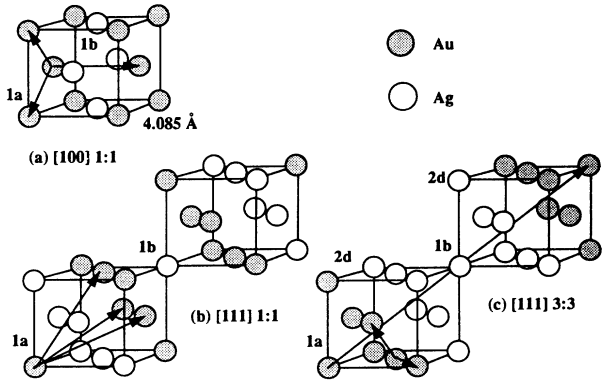

FIG. 1. Unit cells for some Au/Ag multilayers with translational vectors and Wyckoff positions for the atoms. The [100] modulated Au/Ag 1:1 cell (a) is identical to the [110] modulated 1:1 cell. The 1:1 [111] cell (b) and the 3:3 [111] cell (c) are both trigonal.

The procedure for stacking fcc (110) layers to obtain the slab cells neglects some frequently observed aspects of layered materials, namely interdiffusion, surface reconstructure, and interlayer relaxation. Interdiffusion, as

TABLE I. Au/Ag crystallographic data.

Multilayer	n	System	SG	I.T.	Wyckoff position Au; Ag
[100]	1	Tetragonal	D_{4h}^1	123	1a;1b
	2	Tetragonal	D_{4h}^7	129	origin 2:2c, $z=\frac{1}{8}$; $z=\frac{5}{8}$
	3	Tetragonal	D_{4h}^1	123	1a, 2h, $z=\frac{1}{6}$; 1d, 2g, $z=\frac{1}{3}$
[110]	1	Tetragonal	D_{4h}^1	123	1a; 1b (see [100])
	2	Orthorhombic	D_{2h}^{13}	59	origin 2:2a, $z=\frac{1}{8}$; $z=\frac{5}{8}$
	3	Orthorhombic	D_{2h}^1	47	1a, 2t, $z=\frac{1}{6}$; 1h, 2q, $z=\frac{1}{3}$
[111]	1	Trigonal	D_{3d}^5	166	1a; 1b
	2	Trigonal	D_{3d}^3	164	2c, 2d; 2c, 2d
	3	Trigonal	D_{3d}^3	164	1a, 2d, $z=\frac{1}{6}$; 1b, 2d, $z=\frac{2}{3}$
slab		Orthorhombic	D_{2h}^1	47	1a, 1c, 2t, 2q (see Fig. 2)
metal		fcc	O_h^5	225	4a

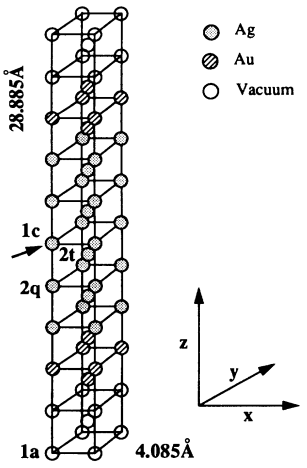

FIG. 2. The basic 11 classes [110] slab (metal-vacuum multilayer) unit cell in the case of 3-Au adlayers. The arrow points to a horizontal mirror plane and the Wyckoff positions of Table I are indicated. The directions (x,y,z) for the labels in Fig. 7 are also presented.

was already mentioned, can be neglected for the Au/Ag system. Although the Au(110) surface is known for its so-called "missing row," or 1×2, surface reconstruction, no reconstructions are reported for Ag(110) or for the few Au monolayers on Ag(110). However, contraction of the interlayer distance between the outermost atomic layers is a real effect, observed for many metallic systems including[4] for Au on Ag(110). Including interlayer relaxations would require time-consuming energy optimizations of the interlayer distances. Since in this first study we are looking for general trends, which are supposed to be not too sensitive to such relaxations, we decided to ignore them.

The space groups (SG) of the structures discussed so far are given in Table I. Their description is based on the "International Tables,"[8] to which the numbers in column I.T. refer. Only the atomic positions for the 3:3 [111] system are given but the positions for the 2:2 system can be derived from the first position given. The positions of the spheres in the slab unit cells can easily be derived from the positions of the 3:3 [110] multilayer. For that reason they are not included in Table I. The last row in Table I gives information about the bulk metals Au and Ag, which were calculated with the lattice parameter 4.085 Å serving as a reference system. For the structures in Table I, which all have the same underlying fcc structure, the radius of the atomic sphere R_{ASA} is 1.5964 Å.

III. CALCULATIONS

Ab initio, self-consistent, LSW calculations[6] using a scalar-relativistic Hamiltonian (no spin-orbit coupling) have been carried out. We used local-density exchange-correlation potentials inside space filling and, therefore, overlapping spheres around the atomic constituents. The self-consistent calculations were carried out including all core electrons.

Iterations were performed with the **k** points distributed uniformly in an irreducible part of the first Brillouin zone, corresponding to a volume of the Brillouin zone per **k** point of the order of 4×10^{-6} Å^{-3}. Self-consistency was assumed when the changes in the local partial charges in each atomic-sphere decreased to the order of 10^{-4}. Subsequently, the densities of states were constructed by solving the Hamiltonian for the same density of **k** points. As sampling histograms, 300 channels with a width of 4.33 mRy were used.

In the construction of the LSW basis,[6] the spherical waves were augmented by solutions of the scalar-relativistic radial equations indicated by the atomiclike symbols $6s,6p,5d$ and $5s,5p,4d$ corresponding to the valence levels of the parent metals Au and Ag, respectively. The internal l summation, used to augment the central Hankel function at surrounding atoms, was extended to $l=3$, resulting in the use of $5f$ orbitals for Au and $4f$ orbitals for Ag. For the vacuum spheres the functions $1s$, $2p$, and $3d$, and, as an extension, $4f$ were used. The screening cluster consists of 12 nearest and 6 next-nearest neighbors, together with the central atom, a total of 19 atoms, giving 162 degrees of freedom for screening the central Hankel functions.

The slabs are a translationally symmetrical approximation for a solid with a surface. For this approximation to be valid, the slabs have to be chosen thick enough to ensure that the innermost layers have all the bulk properties already, thereby ensuring that the slab surfaces do not interact with each other across the slab. Likewise, to prevent the surfaces from interacting across the vacuum, the innermost vacuum layers should have charges and absolute energies smaller than some predescribed value. To accomplish this, the metal-to-vacuum ratio of the number of layers in the slabs was tested for the 14-layer system by varying the number of vacuum layers. It turned out that the spheres in the fourth vacuum layer away from the Ag surface contain less than 10^{-5} electrons and have an associated absolute energy smaller than 0.05 mRy. Therefore we used only five vacuum layers in the calculations of which the central (third) layer contains less than 5×10^{-4} electrons and has an energy of -0.3 mRy. For this choice the central Ag layer, the fifth Ag layer removed from the surface, still does not have the bulk properties. Because the trend toward the bulk values was already visible, and to save computer time, nine Ag layers, with the fifth layer as the central layer, were used as a minimum value for the thickness of the Ag part of the slab. This minimum occurs for the slab with three Au adlayers.

To justify our use of an ASA-based method for calculating a slab supercell we note that such methods, although ideally suited for calculations on close-packed systems, have also been used successfully to describe low-symmetry situations such as a surface.[9] However, the obtained energies for such systems can be rather arbitrary. We feel the use of an ASA-based method for calculating the slab energies is justified in the present work because we keep the ASA radii fixed and use relative energies only.

IV. MULTILAYER RESULTS

A. Density of states

The multilayer density-of-states (DOS) curves are all very similar for different modulation wavelengths and modulation directions. Therefore, we only present the 2:2 [110] DOS in Fig. 3 as an example. The multilayer total DOS can be characterized as a steplike structure extending from -7 to about -2 eV on which, almost in the middle, at -4.5 eV, a sharp peak is superimposed. From -2 eV onward to above the Fermi level, the DOS can, for our purposes, be considered as constant. In the following we will ignore this constant DOS. In Fig. 3(b) the Au contribution, and in Fig. 3(c) the Ag contribution to the total DOS are given, which are to be compared with the DOS of the elemental bulk metals given in Fig. 4(a) for Ag and in Fig. 4(f) for Au. From these we see that the Au DOS, extending from -7.5 to -1.5 eV, is broader than the Ag DOS, which ranges from -6.5 to -2.5 eV. The Au and Ag part of the multilayer DOS extend exactly over the average range, what can be considered as evidence for an Au-Ag interaction. The peak at -4.5 eV in the multilayer DOS has its origin in both bulk DOS curves where it is situated at the same energy level. The Ag DOS contribution to the multilayer differs from the pure Ag DOS in that the peaks at -6 and -3 eV in Fig. 4(a) are greatly reduced, the latter a little bit more than the peak at -6 eV. Au still has the same appearance but there is an intensity shift from the peak at -4.5 eV toward higher energies in Fig. 3(b).

B. Total energy

We investigated the reported bilayer growth of Au on Ag(110) in two different ways. One approach, to be discussed in the following sections, is the direct calculation of Au grown on Ag(110) surfaces, modeled by slabs. The other approach, which we will discuss now, is the calculation of Au/Ag multilayers. In this way we are not only studying the multilayers themselves but we also hope to learn whether there are any correlations between the energies of the multilayers and the occurrence of odd or even numbers of Au layers, which could be evidence for bilayer growth. The total energies of the $n{:}n$ multilayers for the three different growth directions are given in Table II.

We observe from this table that, for the different modulation directions, the energy increases with n. This can be considered as satisfactory regarding the limiting value for large n of -0.2822 Ry, the sum of the energies of the bulk metals with $a=4.085$ Å. Apparently the Au-Ag interaction at the interface has a stabilizing effect on the multilayers. Note, however, that the increase is steady. No effect related to an odd or even number of layers is seen. As for the stabilizing effect, we mention, in addition, that a raise in Au energy and a lowering in Ag energy is found relative to the energies of the elemental metals whose explicit values are given in Sec. VI. For instance, in the 3:3 [110] multilayer, an increase of 0.0292 and 0.0130 Ry is found for the Au bulklike and interface atoms, respectively. The Ag atoms show a decrease of -0.0353 and -0.0143 Ry for the bulklike and interface

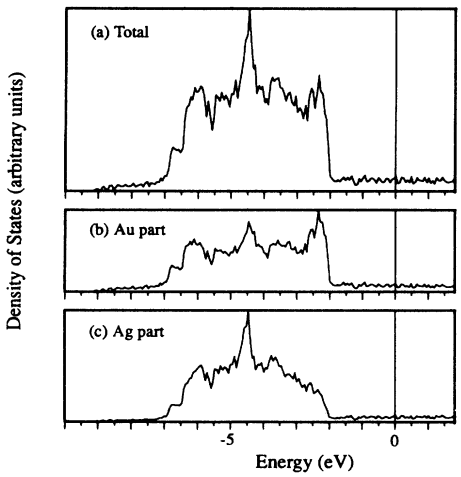

FIG. 3. Density-of-states curves for the Au/Ag 2:2 [110] multilayer; (a) total DOS, (b) the Au contribution, and (c) the Ag contribution. The horizontal axis is in electron-volts (eV) relative to the Fermi energy and the vertical axis is in arbitrary units.

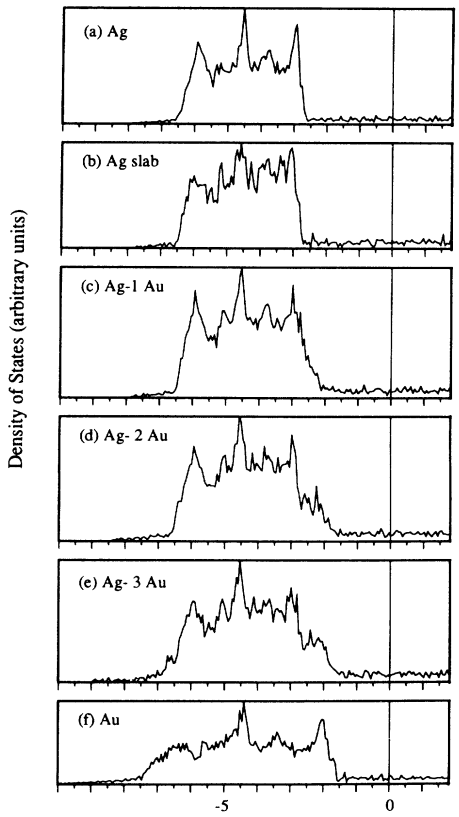

FIG. 4. Density of states for Ag slabs with different Au coverages and for the bulk metals (a) Ag and (f) Au. The Ag slab is given in (b) followed by Ag slabs covered by one (c), two (d), and three (e) monolayers of Au. The axes of the figures are as in Fig. 3.

TABLE II. Total energies (Ry per Au/Ag pair), increased with 48 624 Ry. The number of Au-Ag nearest neighbors for atoms in different layers is given between parentheses.

n	[100]		[110]		[111]	
1	−0.2906	(8)	−0.2906	(8)	−0.2884	(6)
2	−0.2865	(4)	−0.2885	(6)	−0.2859	(3)
3	−0.2853	(0,4)	−0.2869	(2,5)	−0.2847	(0,3)

atoms, respectively. The effect on Ag is larger, resulting in an overall energy lowering. The contribution of the individual metals to the Au-Ag interaction as mentioned here could already be observed in the comparison between the elemental Ag and Au DOS curves in Figs. 4(a) and 4(f) and the multilayer DOS curve in Fig. 3. The multilayer Au part has an increased intensity in the high-energy region of the *d* band (antibonding) and the Ag part has its strongest decrease in this region.

These energies can be analyzed further by counting the number of unlike nearest neighbors (NN) of the atoms in the different geometries. The 12 NN of an atom in a fcc lattice are decomposed in Table III according to direction and covering layers.

Combining the numbers in Table III with the energies of the multilayers of Table II, a strong relation between the number of Au-Ag NN and the total energy of the multilayer emerges, indicating the stabilizing effect of Au-Ag bonding. The 3:3 systems can be compared with the other systems by dividing the total number of Au-Ag NN positions in the cell by 3, the number of Au-Ag pairs in the 3:3 cells. We then find the numbers $2\frac{2}{3}$, 4, and 2 for the [100], [110], and [111] 3:3 systems, respectively. So instead of a sought-for odd-even correlation, we find a correlation based on the occupation of NN atomic positions by unlike atoms. From the difference between the results of Table II and the limiting value for large n the magnitude of the Au-Ag interaction can be estimated to be of the order of 1 mRy per atomic pair. This is a fair estimate because structural energies can be neglected in this system. However, there are some inaccuracies inherent in the various aspects of the method, such as the overlap of the spheres and the inability to account for nonspherical contributions to the energy. A measure of their influence is the total-energy difference of 0.4 mRy between the 2:2 [100] and the 3:3 [110] system that both have 4 Au-Ag NN. It is likely that the electronic similarity of the metals Au and Ag and the overall fcc environment causes this energy difference to be that small. A similar observation can also be made for the Nb/Ta multilayer system.[10] The negative interaction energy for the Au-Ag system is consistent with a conjecture that the interface energy of Au and Ag is small but negative[11] and with the small but negative heat of mixing reported for Au-Ag alloys.[12] Reference 13 reports small but negative heat-of-mixing values for Au and Ag that have a minimum of −4.66 kJ/mol (−3.5 mRy/atom) at a 50:50 mixing ratio.

TABLE III. NN in fcc metal.

Layer	0	1	2
[100]	4	4	
[110]	2	4	1
[111]	6	3	

V. SLAB DENSITY OF STATES

The total DOS curves for the pure and Au-covered Ag slabs are presented in Figs. 4(b)–4(e), together with the DOS curves of the metals Ag [4(a)] and Au [4(f)]. When going from panel (c) to panel (e) we clearly see the effects of the increased Au content superimposed on the peaks of Ag at −6, −4.5, and −3 eV that still comprises the major part of the slabs. Figure 4(e) bears some resemblance to Fig. 3(a) for the multilayer, but for the slab configuration the Ag and Au curves are essentially added instead of being deformed by mutual interactions. However, simply adding bulk DOS curves is too naive an approach to the slab DOS curves, which is most directly seen by comparing Figs. 4(a) and 4(b). Clearly, it is the metal/vacuum interface, and for the Au-covered systems also the Au/Ag interface, that need to be included in the discussion.

To see the effect of the interfaces on the metal DOS, we consider the layer-resolved curves of the pure Ag slab in Fig. 5 and of the Ag slab covered by one monolayer of Au in Fig. 6. The curves for the slabs with more Au layers are not given because no essential additional effects

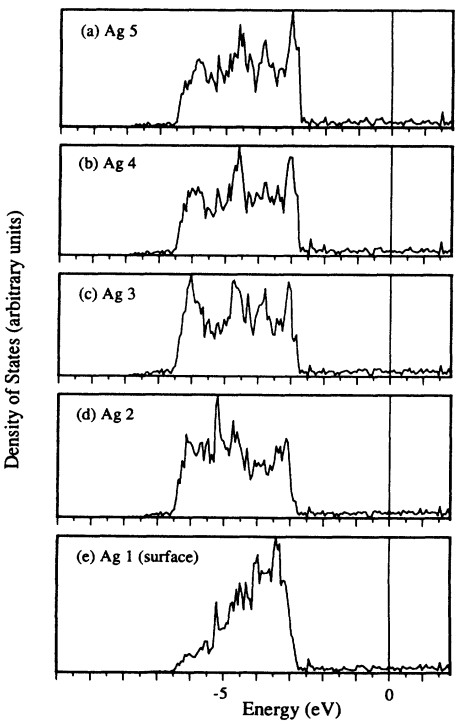

FIG. 5. Layer-resolved density of states of the Ag slab of Fig. 4(b). The layers are numbered counting away from the vacuum interface. (a) gives the central Ag layer and (e) the surface Ag layer. The axes of the figures are as in Fig. 3.

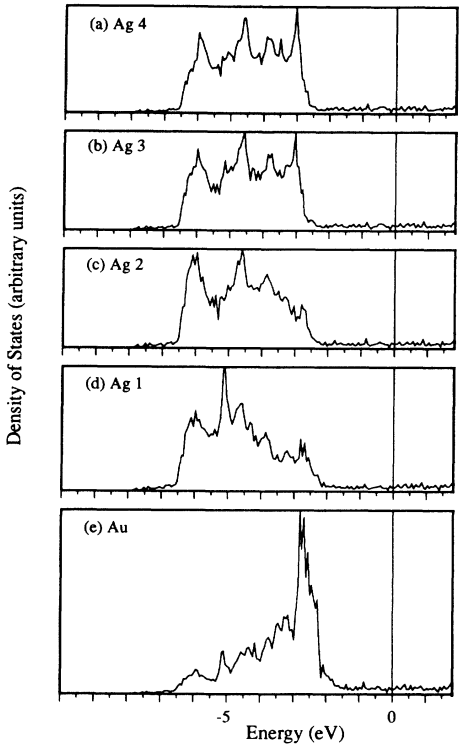

FIG. 6. Layer-resolved density of states of the Ag slab covered by one monolayer of Au of which the total DOS is given in Fig. 4(c). The Ag layers are numbered counting away from the Au layer. Plots for the fifth to seventh Ag layers are omitted. The axes of the figures are as in Fig. 3.

are observed compared with those which are already present in Figs. 5 and 6. Trends to be read from Figs. 5 and 6, supported by results for the slabs with more Au adlayers, will be mentioned, however.

The following observations are made. (i) The third Ag layer counted from an interface, with Au or with the vacuum, already resembles Ag bulk. If there are two or three Au layers between Ag and vacuum, then the second Ag layer already starts to resemble bulk Ag. (ii) Every second metallic layer away from the vacuum, Ag or Au, has a sharp peak in its DOS at about -5.2 eV. Therefore, this peak has to be induced by the surface, and will be studied in some more detail in the next paragraphs. (iii) Moving from the Fermi energy toward lower energies the DOS curves of the surface atoms have a rather steep rise at about -2.7 eV for Ag and at -2.2 eV for Au, after which the DOS gradually falls off. In all slabs the DOS curves for the surface atoms show this roughly triangular shape. (iv) Another strong effect can be observed in the first and second Ag layers in Fig. 6, where the DOS at higher energies is reduced relative to the bulk DOS. This is also observed for the second Ag layer in the pure Ag slab [Fig. 5(d)] and the first Ag layer in the slab covered with two Au layers. This effect corresponds to situations where the Ag layers are connected, in a NN sense, to an interface with either Au or vacuum.

The origin of the changes in the metal DOS curves near the vacuum interface can be studied from Fig. 7. In this figure we have plotted the metal d states for the first three layers in the pure Ag slab decomposed according to the magnetic quantum number m. The decomposition labels are indicated at the left of Fig. 7 and the x, y, and z directions are defined in Fig. 2. Note that the two NN atoms in the (110) plane lie on the x axis.

The results of the third Ag layer will be used as a reference to understand the development of the states toward the surface. The curves for this layer can be grouped, taking together those for the orbitals d_{yz} and d_{xy} on one hand and those for the orbitals $d_{x^2-y^2}$, d_{xz}, and d_{z^2} on the other. The former have common peaks at about -3.7 eV; the latter, around -4.5 and -3 eV. We will ignore the small difference between the structures that both groups have around -6 eV. The latter orbitals, with the exception of d_{xz}, further have in common that they have the largest overlap with the NN sites. The second layer, which has one NN position in the vacuum, already shows marked differences as compared to the curves of the third layer. The peak at -5.2 eV which was absent in the curves for the third layer but is observed for all second-

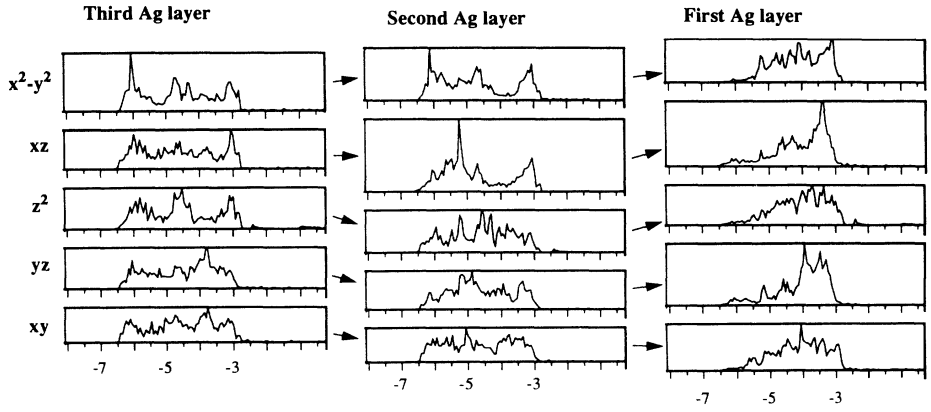

FIG. 7. The m-resolved d density of states of the three Ag layers closest to the surface of the pure Ag slab for which the layer-resolved DOS curves are given in Fig. 5. The first layer is closest to the surface of the slab. Only the energy region of interest is shown.

layer DOS curves in Fig. 4, is very pronounced in the d_{xz}, d_{yz}, and d_{z^2} curves. All the corresponding orbitals have a component in the direction of the surface. The peak at −5.2 eV is clearly missing in the d_{xy} curve and for the $d_{x^2-y^2}$ it is not certain whether it exits. The curves for the latter two orbitals, having their lobes lying parallel to the surface and being more suited to retain their bulklike character, have suffered only minor changes on going from the third layer to the second layer. In the curves of the first layer, the −5.2-eV peak is also present, but it is smaller than for the second layer. This observation suggests that this peak is not induced by a metal-vacuum interaction but by an increased interaction between the first and second layer. For completeness we note that the vacuum DOS is not given because it hardly has any intensity or structure and also does not show a −5.2-eV peak. The fact that the intensity of the −5.2-eV peak is higher for the second layer than for the first layer, which is seen most clearly in the layer-resolved curves of Figs. 5(d) and 5(e), indicates that the center of the interaction is closer to the second layer. This is in agreement with the observation that the surface interlayer distance of many metallic systems contracts with respect to the interlayer distances as found in the bulk, which is also the case for the present system.[4]

A final point to discuss is the position of the peaks with highest intensity in the surface and second-layer curves. As is readily noted, the curves with a z component have in the second layer their highest intensity between the center and the bottom of the DOS and in the surface layer between the center and the top of the DOS. A plausible explanation for these observations lies in the bonding-antibonding hybridization of the Ag orbitals adapted to the reduced symmetry of the interface. Orbitals that in the bulklike layers, like the third layer, contribute to the central energy region of the DOS curves, are transformed to bonding orbitals contributing to the low-energy region in the second layer DOS curves. In this way the bonding between the second layer and the interface layer is increased. The same mechanism, used now to avoid bonding towards the vacuum by using antibonding orbitals, explains the positions and intensity of the surface layer curves. From comparison with calculations on Cu(001) films by Smith, Gay, and Arlinghaus,[14] the observed behavior of the DOS of the surface layer is apparently a quite general result. In the Cu calculations also, a skewed DOS is found for the surface layer, which is explained as being caused by surface states. It is of interest to note that in Fig. 12 of Ref. 14 there is also a low-energy peak in the second layer DOS curve, just as in our results. It is not clear whether the origin of these peaks is the same, as it was not discussed in their work.

VI. SLAB TOTAL ENERGY

In Table IV the energies for the different layers of the slabs are presented. We start with discussing the results for the Ag parts of the slabs. It is seen that the deviations from bulk Ag are largest for the layers closest to the interface. Ag layers 1 and 2 in the pure Ag slab, and the first Ag layer in the 1-Au-layer slab, have a large and pos-

TABLE IV. Energy differences (Ry) for the layers in the slabs relative to the bulk values, being −38 002.0531 Ry for Au and −10 622.2291 Ry for Ag. The layers are numbered separately for Ag, Au, and the vacuum spheres (v.s.), counting away from the metal-vacuum interface. The pure Ag column represents the data of the pure Ag slab. Subsequent columns give the data for the Au-covered slabs in order of increasing number of adlayers. In all slabs the third vacuum layer has a constant energy value of −0.3 mRy and was excluded from the table.

		Pure Ag	Ag/1-Au	Ag/2-Au	Ag/3-Au
Ag	7		−0.0083		
	6		−0.0094	−0.0078	
	5	−0.0176	−0.0082	−0.0087	−0.0066
	4	−0.0214	−0.0119	−0.0071	−0.0069
	3	−0.0147	−0.0176	−0.0113	−0.0069
	2	0.0551	−0.0147	−0.0245	−0.0194
	1	0.2556	0.0375	−0.0441	−0.0553
Au	3				0.0198
	2			0.1037	0.0796
	1		0.3326	0.3137	0.3087
v.s.	1	−0.1392	−0.1664	−0.1768	−0.1771
	2	−0.0211	−0.0285	−0.0285	−0.0282
Ag_{tot1}		0.2570	−0.0149	−0.0957	−0.0951
Ag_{tot2}		0.2369	−0.0149	−0.0870	−0.0816
Au_{tot}			0.3326	0.4174	0.4081
$v.s._{tot}$		−0.1603	−0.1949	−0.2053	−0.2053
Total 1		0.097	0.123	0.116	0.108
Total 2		0.077	0.123	0.125	0.121

itive deviation from the bulk Ag energy. Clearly, the Ag-vacuum interface raises the energy of the Ag layers in NN contact with the vacuum, an effect that will be seen for the Au-vacuum interface as well. (We shall return to this issue in the discussion of the total Ag energies.) The large and negative energies of the first Ag layers in the 2-Au-layer and 3-Au-layer slabs are caused by the screening of the vacuum by the Au adlayers and the stabilizing Au-Ag interaction. For the deeper-lying layers we see that bulk Ag is approached differently in the various slabs. For the Ag, 1-Au-layer, and 2-Au-layer slabs we see a weak oscillatory behavior of the energy difference for the innermost Ag layers. For the 3-Au-layer slab there is only a gradual increase.

In none of the slabs is bulk Ag really reached for the central layer in the sense that the energy differences with bulk Ag vanish. This means that the slabs, strictly speaking, are still not thick enough, which leads to some ambiguity when determining the energy difference between an Ag surface and bulk Ag from our slab results. In a first approach to this energy difference we take just the first five Ag layers in every system, which gives the Ag_{tot1} results. However, the differences between the Ag_{tot1} values of the 2-Au-layer and 3-Au-layer slabs are much smaller than the deviations from bulk energy of the Ag layers not included. This makes conclusions from Ag_{tot1} values rather speculative. As an alternative approach we sum the energy deviations of the Ag layers to the same level of approximation in each of the slabs, thereby hoping that the sum of the energy contributions of the neglected layers are all the same. The results of this procedure, indicated by Ag_{tot2}, are obtained as follows. Counting from the surface inward, 7, 5, 4, and 3 Ag layers were used for the columns from left to right, respectively. The energies for the sixth and seventh layers of the pure Ag slab were supposed to be given by the energies of the fourth and fifth layers of the 1-Au-layer slab. This procedure, although more accurate than just taking five Ag layers for all slabs, still has a great deal of arbitrariness. We now have a truncation at an energy difference of about -7 mRy. For this choice, comparing the different systems, the relative uncertainty is estimated to be at least 5 mRy. Due to the necessity of a truncation an absolute uncertainty remains as large as the energy tail that is not included.

Despite the differences between the Ag_{tot} values a strong relation emerges between the energy of the Ag part and the number of Au adlayers atop in the form of two distinct steps in the Ag_{tot} energies. These steps can be understood from the fact that a fcc (110) surface is affected two layers deep by neighboring layers. The first step occurs when going from the Ag slab to the 1-Au-layer slab where there is one layer of Ag-vacuum interactions replaced by Ag-Au interactions. The second step occurs when going from the 1-Au-layer slab to the 2-Au-layer slab, eliminating all Ag-vacuum NN pairs, after which the energy of the Ag part stabilizes.

The Au adlayers show the same trend as the Ag layers. The effects are strongest at the vacuum interface and diminish when moving away from the interface. However, the energy difference for the first Au layer is significantly larger than for the first Ag layer. The third Au layer in the 3-Au-layer system has only metallic NN and still the energy difference with bulk Au is positive. This can be understood by considering the Ag-Au interaction effect. We have seen for the multilayers that in the Ag-Au interaction the energy of the Ag atoms is lowered and, to a lesser extent, the energy of the Au atoms is raised, resulting in a stabilizing overall Au-Ag interaction. Apparently this is a contributing factor here also. The positive Au energy for the third layer, an effect which is not seen for the third layer of the pure Ag slab, is counterbalanced by a large negative energy for the first Ag layer. This can also be inferred from the similarity of the Au_{tot} energies of the 2-Au-layer and 3-Au-layer slabs. The second Au layer in the 2-Au-layer system is raised in energy by interactions both with vacuum and with Ag. The second Au layer in the 3-Au-layer system is less influenced by Ag but is still as much influenced by vacuum as layer 2 is in the 2-Au-layer system, and as a consequence its energy is lower. The third Au layer in the 3-Au-layer slab is only influenced by Ag and no longer by the vacuum and, as a result, shows an energy increase caused mainly by its interaction with Ag. Therefore, it is not surprising that the sum of the energy deviations of layers 2 and 3 of the 3-Au-layer system is only 4.3 mRy smaller than the energy deviation of the second Au layer in the 2-Au-layer system.

It is seen that the vacuum spheres (v.s.) close to the metal surface also contribute to a lowering of the total energy of the system, and that they contribute somewhat more for the Au-covered slabs than for the pure Ag slab. A further interesting effect is the considerable amount of electronic charge that is transferred from the metal to the vacuum. The first layer of vacuum spheres receives most of the electrons. The spheres at the Ag surface gain 0.28 electrons and those in contact with the Au layers gain 0.32 electrons in case of the 1-Au-layer system and 0.33 electrons for the 2-Au-layer and 3-Au-layer systems. This electron density gain drops very fast on going away from the metal surface. For all slabs, the third (central) vacuum layer spheres already contain less than 5×10^{-4} electrons.

In the last two lines of Table IV the energies representing the sum of the Ag_{tot}, Au_{tot}, and $v.s._{tot}$ energies are given. Before discussing these energies, we want so summarize the trends and the competing effects that make up the total energy. First, the energies of the metal and vacuum layers follow a similar behavior as electron density variations behave in the jellium model for a metal surface: exponential decay into the vacuum and (Friedel) oscillations toward bulklike behavior into the metal. Second, there is the destabilizing effect of the metal-vacuum interface, which is larger for Au than for the Ag surface. This is in accordance with values for surface free energies[15] which are $\gamma_{Au}=1.6$ J/m^2 and $\gamma_{Ag}=1.3$ J/m^2. The difference between an Ag and an Au surface is also obvious from the observed 1×2 surface reconstruction of the Au(110) surface. This reconstruction is observed neither for the Ag(110) surface nor for the (few) Au(110) monolayers on Ag(110).[4] Third, the Au-Ag interaction has a stabilizing effect, as was already clear from the

Au/Ag multilayer calculations of Sec. IV B. Fourth, the stabilization caused by the vacuum layers is larger for Au than for Ag, as is seen from $v.s._{tot}$. Finally, if the number of Au layers is increased, the system with two Au adlayers is most unstable when we look at the Au_{tot} energies only. For this system there is no Au background as is the case in the 3-Au-layer system and two Au layers are in contact with the vacuum instead of one, as in the 1-Au-layer system.

Regarding the total energies it is useful to make a connection with the work of Weinert *et al.*,[16] who studied adsorbed layer and multilayer materials for the case of Pd and Ag on different Nb surfaces. The energetics of adlayer behavior can be disentangled as

$$\Delta E=\gamma_{ad}-\gamma_{substr}+\xi+\Delta E_{str} , \quad (1)$$

where $\gamma_{ad}-\gamma_{substr}$ is the difference in surface energy between having a surface of *adsorbate* rather than a pure *substrate* surface, ξ is the energy associated with bonding at the interface, and ΔE_{str} is the structural energy cost to provide registry between adsorbate and substrate. In view of this expression, the advantage of the Au/Ag system is seen in that ΔE_{str} can be neglected because of the almost perfect match of the lattices. As a result the atoms at the metallic interface contribute to ξ only. The energetics of the multilayer system can then be written as

$$\Delta E=2\xi , \quad (2)$$

since there are two metallic interfaces per unit cell and no free surfaces.

The various contributions to Eq. (1) can be estimated or directly be derived from the present calculations. Clearly, the large electronic reorganization that takes place at a metal-vacuum interface can cause differences in both sign and magnitude of the charge transfer in a multilayer interface with that in a substrate-adlayer interface. For multilayers with large modulation wavelengths and substrates with thick epitaxial coverages, these interfaces become equal, and Eqs. (1) and (2) can be applied. From a comparison between the layer-resolved energies of the 3:3 [110] multilayer and, for instance, those of the 3-Au system, it is clear that using ξ determined from the multilayers is only an estimate for the Au-Ag interaction of Au monolayers on the Ag(110) surface.

Using Eq. (2), we can find an estimate for ξ for the different Au-Ag interfaces from Table III and the interaction energy per Au-Ag NN pair of -1 mRy. This simple approach for the (110) interface gives for ξ a value of -6 mRy/atom for the first Au interface layer. (There are five Ag-Au NN pairs for the first layer and one for the second interface layer.) Furthermore, we use the total energy of the Ag slab as an estimate of the surface energy of the Ag(110) surface. The *Total* 2 result, 77 mRy/atom, corresponds to a value of 1.05 eV/atom (1.4 J/m^2) which is in good accord with previously calculated values of 1.0 eV/atom (Ref. 16) and 1.13 eV/atom.[17] The neglected terms of the Ag_{tot} energies would further decrease this number. The *Total* 1 value is about 26% larger than the *Total* 2 value. No separate Au(110) slab calculation to access γ_{Au} was performed. The stability of the *Total* 2 energies for the Au-covered slab allows for an estimate of γ_{Au} of about 0.12 Ry/atom. In this estimate the interface energy ξ has been neglected.

The total energies *Total* 1 and *Total* 2, though depending on how the Ag energies are counted, clearly reflect the domination of the surface energies over the interface bonding term ξ, and thereby determine the overall energetics of the adlayer systems. Therefore, a Frank–van der Merwe growth mode of Au on Ag(110) is unlikely to be observed, which is in agreement with the experimental data that report islanding. It is clear that it is more favorable to have a pure Ag surface than an Au-covered Ag surface. Furthermore, as the total energy is rather invariant for the number of Au layers added, islanding must be preferred because it is better for newly added Au atoms to cover Au than Ag. To explain the observed bilayer growth we return to the Ag_{tot} energies where we have discussed the occurrence of two steps in the energy associated with the substitution of vacuum by Au at an Ag NN position. For complete monolayer coverages, as we have calculated, the energy is rather invariant to the number of Au layers on top of the Ag surface. However, for individual Au atoms impinging on and moving along the Ag surface, the "dangling Ag NN bond" could well provide an additional pinning center for first- as well as for second-layer Au atoms, thereby favoring bilayer growth. The fact that no 1×2 reconstruction is observed for the first few adlayers of Au is also understandable from this argument. Thus it could well be possible for the initial growth of Au on Ag(110) to occur via bilayers, but only for the first two layers which have an Au-Ag NN interaction, due to the open geometry of the Ag(110) surface. Subsequent growth of Au bilayers is expected to be highly improbable, however.

VII. CONCLUSIONS

The total energies of the Au/Ag multilayers for the three growth directions can be ordered according to a nearest-neighbor scheme in which the Au-Ag NN pairs are counted. This observation allows us to assign a negative energy of about -1 mRy per Au-Ag NN pair in Au/Ag multilayers. A small but negative Au-Ag interaction is known from literature.[11,12] The DOS curves of the Au/Ag multilayers are all quite the same and no changes at the Fermi level are observed. The individual Au and Ag contributions to the multilayer DOS reflect the Au-Ag interaction.

Slab calculations were performed without surface reconstruction or interlayer relaxation. Although the associated energy effects are expected to influence the total-energy results, trends from the calculations neglecting these effects are supposed to be rather insensitive to it.

The local DOS curves for the slabs show a peak localized between the first and second surface layer and a shift in *d*-state density to higher energies at the interface and to lower energies for the layer below the interface as compared with the elemental DOS curves. From the analysis of the *d* DOS of the Ag slab layers, resolved for magnetic quantum number, these peaks are assigned to *d* orbitals which have their spatial extensions in the direction of the surface.

From the total-energy calculations on the slabs it is found that the energy of a bare Ag(110) surface is lower than that of an Ag(110) surface covered by Au monolayers. This is in agreement with the difference between Ag and Au surfaces in general. The fact that islanding of Au on Ag(110) is observed implies that the Au-Ag (interface) bonding energy is dominated by the difference in surface energy of the metals. This is supported by our calculations. On an atomic scale however, the negative interface energy is thought to be responsible for the observed Au bilayer growth in islands on Ag(110). The open geometry of the (110) surface allows for nearest-neighbor positions in two adjacent (110) layers. This way, Au atoms in the top Au adlayer in a two-layer coverage can still gain interface energy. Second adlayer positions are thereby favored over positions in layers more distant from the Ag surface. On the basis of our total-energy results, we therefore suggest a mode where one bilayer is deposited in separated domains before 3D islanding commences.

ACKNOWLEDGMENTS

The authors would like to thank Professor J. E. Inglesfield for critically reading the manuscript. This work is part of the research program of the Stichting voor Fundamenteel Onderzoek der Materie (FOM), which is financially supported by the Nederlandse Organisatie voor Wetenschappelijk Onderzoek (NWO).

[1]T. C. Hsieh, A. P. Shapiro, and T.-C. Chiang, Phys. Rev. B **31**, 2541 (1985).

[2]T. Miller, M. A. Mueller, and T.-C. Chiang, Phys. Rev. B **40**, 1301 (1989).

[3]R. J. Culbertson, L. C. Feldman, P. J. Silverman, and H. Boehm, Phys. Rev. Lett. **47**, 657 (1981).

[4]P. Fenter and T. Gustafsson, Phys. Rev. Lett. **64**, 1142 (1990).

[5]P. Fenter and T. Gustafsson, Phys. Rev. B **43**, 12 195 (1991).

[6]H. van Leuken, A. Lodder, M. T. Czyżyk, F. Springelkamp, and R. A. de Groot, Phys. Rev. B **41**, 5613 (1990).

[7]A. R. Williams, J. Kübler, and C. D. Gelatt Jr., Phys. Rev. B **19**, 6094 (1979).

[8]*International Tables for Crystallography, Vol. A: Space Group Symmetry,* edited by T. Hahn (Reidel, Dordrecht, 1983).

[9]G. Y. Guo, J. E. Inglesfield, M. Arnott, and W. M. Temmerman, J. Phys. Condens. Matter **1**, SB241 (1989).

[10]H. van Leuken, A. Lodder, and R. A. de Groot, J. Phys. Condens. Matter **3**, 3945 (1991).

[11]E. Bauer, Appl. Surf. Sci. **11**, 479 (1982).

[12]*Metals Reference Book,* edited by C. J. Smithells (Plenum, New York, 1967), Vol. 1, p. 232.

[13]O. Kubaschewski, in Landolt-Börnstein, Vol. II, Pt. 4, edited by Kl. Schäfer and E. Lax (Springer-Verlag, Berlin, 1961), p. 807.

[14]J. R. Smith, J. G. Gay, and F. J. Arlinghaus, Phys. Rev. B **21**, 2201 (1980).

[15]L. Z. Mezey and J. Giber, Jpn. J. Appl. Phys. **21**, 1569 (1982).

[16]M. Weinert, R. E. Watson, J. W. Davenport, and G. W. Fernando, Phys. Rev. B **39**, 12 585 (1989).

[17]J. R. Smith and A. Banerjea, Phys. Rev. Lett. **59**, 2451 (1987).

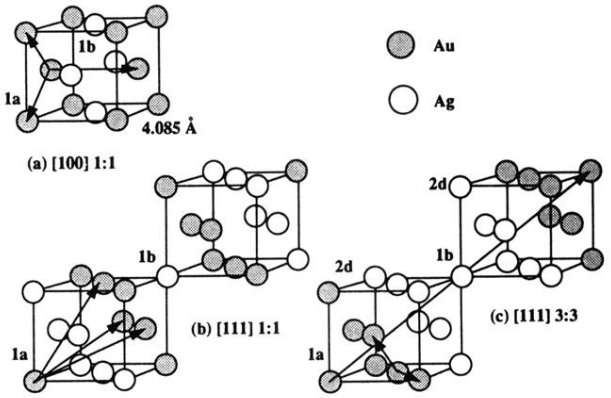

FIG. 1. Unit cells for some Au/Ag multilayers with translational vectors and Wyckoff positions for the atoms. The [100] modulated Au/Ag 1:1 cell (a) is identical to the [110] modulated 1:1 cell. The 1:1 [111] cell (b) and the 3:3 [111] cell (c) are both trigonal.

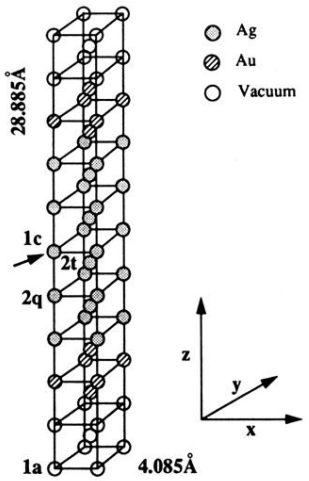

FIG. 2. The basic 11 classes [110] slab (metal-vacuum multilayer) unit cell in the case of 3-Au adlayers. The arrow points to a horizontal mirror plane and the Wyckoff positions of Table I are indicated. The directions (x,y,z) for the labels in Fig. 7 are also presented.